

Revealing the topological nature of the bond order wave in a strongly correlated quantum system

Sergi Julià-Farré ^{1,*} Daniel González-Cuadra,^{1,2,3} Alexander Patscheider,⁴ Manfred J. Mark,^{3,4} Francesca Ferlino,^{3,4} Maciej Lewenstein,^{1,5} Luca Barbiero ^{6,1} and Alexandre Dauphin ^{1,†}

¹*ICFO - Institut de Ciències Fòniques, The Barcelona Institute of Science and Technology, Av. Carl Friedrich Gauss 3, 08860 Castelldefels (Barcelona), Spain*

²*Center for Quantum Physics, University of Innsbruck, 6020 Innsbruck, Austria*

³*Institut für Quantenoptik und Quanteninformation, Österreichische Akademie der Wissenschaften, Technikerstraße 21a, 6020 Innsbruck, Austria*

⁴*Institut für Experimentalphysik, Universität Innsbruck, Technikerstraße 25, 6020 Innsbruck, Austria*

⁵*ICREA, Pg. Lluís Companys 23, 08010 Barcelona, Spain*

⁶*Institute for Condensed Matter Physics and Complex Systems, DISAT, Politecnico di Torino, I-10129 Torino, Italy*



(Received 13 January 2022; revised 19 April 2022; accepted 14 June 2022; published 8 July 2022)

We investigate the topological properties of the bond order wave phase arising in the extended Fermi-Hubbard model. In particular, we uncover a topological sector, which remained elusive in previous finite-size numerical studies due to boundary effects. We first show that, for an infinite system, the bond order wave regime is characterized by two degenerate bulk states corresponding to the trivial and topological sectors. The latter turns out to be indeed characterized by an even degeneracy of the entanglement spectrum and long-range order of a string correlation function. For finite-size systems, we show that the topological sector can be stabilized by imposing a suitable border potential. This therefore provides a concrete protocol for the observation of topologically protected degenerate edge modes in finite-size systems. Furthermore, we show that the bulk of the system is characterized by exotic solitonic solutions interpolating between the trivial and topological sectors. Finally, we propose an implementation and detection scheme of this strongly correlated topological phase in a quantum simulator based on dipolar Fermi gases in optical lattices.

DOI: [10.1103/PhysRevResearch.4.L032005](https://doi.org/10.1103/PhysRevResearch.4.L032005)

Introduction. In the recent years, great effort has been devoted toward the study of symmetry-protected topological (SPT) phases [1–5]. These exotic phases, characterized by nonlocal order parameters, escape the conventional Ginzburg-Landau theory of phases of matter [6,7], and their robustness with respect to local perturbations allows for applications going from metrology to quantum computation [8,9]. Owing to their high level of control [10,11], ultracold atomic systems represent an ideal platform where such intriguing states of matter can be investigated [5,12]. In one dimension, one of the most paradigmatic models hosting a SPT phase, the Su-Schrieffer-Heeger (SSH) model [13], has been realized in atomic quantum simulators [14,15] and its robustness to disorder has been probed [16]. While these experiments probed noninteracting models, the inclusion of interactions can lead to much richer phenomena [17,18].

Furthermore, SPT phases can arise directly from interactions, as it is the case of the original SSH Hamiltonian in

polyacetylene. There, a bond order wave (BOW) arises spontaneously from the coupling between electrons and phonons through a Peierls mechanism [19], which can also occur in spin-boson models [20–22]. Interestingly, similar BOW phases also appear in interacting single-species systems, induced by frustration between competing orders [23–43], including strongly correlated electrons, quantum magnets, or ultracold atomic systems. Although the insulating nature and effective dimerization of these systems have been very carefully characterized, their topological nature still needs to be unveiled. The latter requires an accurate analysis of such many-body interacting systems, as the sole presence of a spontaneous dimerization, i.e., a local order parameter, does not directly translate into a nontrivial topology.

In this Letter, we reveal and characterize the SPT nature of such BOW phases arising from frustration in the presence of chiral symmetry [26–43]. Moreover, we propose a realistic implementation and detection scheme for the realization of the frustration-induced topological BOW phase with dipolar gases in optical lattices. Our proposal allows us to go beyond the experimental simulation of noninteracting SPT phases, promising to access both bulk and edge physics of a strongly correlated topological phase with richer phenomenology.

More specifically, we focus our analysis on the one-dimensional (1D) extended Fermi-Hubbard (EFH) model. We demonstrate that, in the case of an infinite chain, two exactly degenerate BOW ground states occur. These states are

*sergi.julia@icfo.eu

†alexandre.dauphin@icfo.eu

Published by the American Physical Society under the terms of the [Creative Commons Attribution 4.0 International](https://creativecommons.org/licenses/by/4.0/) license. Further distribution of this work must maintain attribution to the author(s) and the published article's title, journal citation, and DOI.

invariant under chiral and bond-inversion symmetries, and correspond to the topological and the trivial ground states of the interacting SSH model [44–51]. As indeed required by SPT phases, we find that the topological state is characterized by the long-range order of a specific nonlocal string correlator [52–54] and by an even degeneracy of the entanglement spectrum (ES) [3,55]. Furthermore, we show that, in a finite-size system, the topological sector of the BOW can be stabilized by means of a suitable local pinning. In this case, the *bulk-edge* correspondence of SPT phases translates into the presence of gapless spin edge modes that were not observed in previous finite-size studies. Exemplary to the rich phenomenology of the system, we find that further spin bulk excitations create solitonic structures interpolating between the topological and trivial sectors of the BOW.

Finally, we propose an experimental setup based on erbium magnetic atoms trapped in a 1D optical lattice. Impressive steps forward have been achieved in ultracold systems made of magnetic atoms with large dipolar momenta to simulate large and nonlocal interactions [56]. The peculiar nonlocal dipolar repulsion has made possible the experimental study of exotic states of matter, such as droplet liquids [57,58] and supersolids [59–62], as well as the investigation of ergodic behaviors [63]. Furthermore, it has been also experimentally demonstrated that, when trapped in a lattice, magnetic atoms mimic the physics of extended Hubbard Hamiltonians [64–69]. As we reveal, such a setup allows, on one side, to have sizable nonlocal repulsion required to achieve the BOW regime and, on the other, to perform very accurate measurements of density distribution and string correlators through a quantum gas microscope [70–73].

Extended Fermi-Hubbard model. The EFH model describes a chain of length L where N spinful fermions, labeled by $\sigma = \uparrow, \downarrow$, interact through contact and nearest-neighbor (NN) repulsion. The Hamiltonian modeling such a system reads as

$$\hat{H} = -t \sum_{(ij),\sigma} (\hat{c}_{i,\sigma}^\dagger \hat{c}_{j,\sigma} + \text{H.c.}) + U \sum_{i=0}^{L-1} \hat{n}_{i,\uparrow} \hat{n}_{i,\downarrow} + V \sum_{(ij)} \hat{n}_i \hat{n}_j, \quad (1)$$

where t parametrizes the NN hopping, U accounts for the on-site Hubbard interaction, and V describes the repulsion between fermions in NN sites. Here, we restrict our investigation to the case where both N and the total magnetization $\hat{S}_z \equiv \sum_i (\hat{n}_{i,\uparrow} - \hat{n}_{i,\downarrow})/2$ are conserved and, unless specified, we consider the half-filled case with $N = L$ and $\hat{S}_z = 0$. We emphasize that, for spinful fermionic systems, both charge and spin degrees of freedom have to be considered. More precisely, we refer to a gapped charge or spin sector when the system has to pay a finite energy for adding/removing an up-down pair, or flipping a single fermion, respectively.

Phase diagram. When U dominates the system is a Mott insulator (MI) with a finite charge gap and short-range antiferromagnetic order. Alternatively, for large V the system has a fully gapped charge density wave (CDW), characterized by an effective antiferromagnetic order, with alternating empty and doubly occupied sites. In the strongly interacting limit $U, V \gg t$ there is a direct transition between these two phases

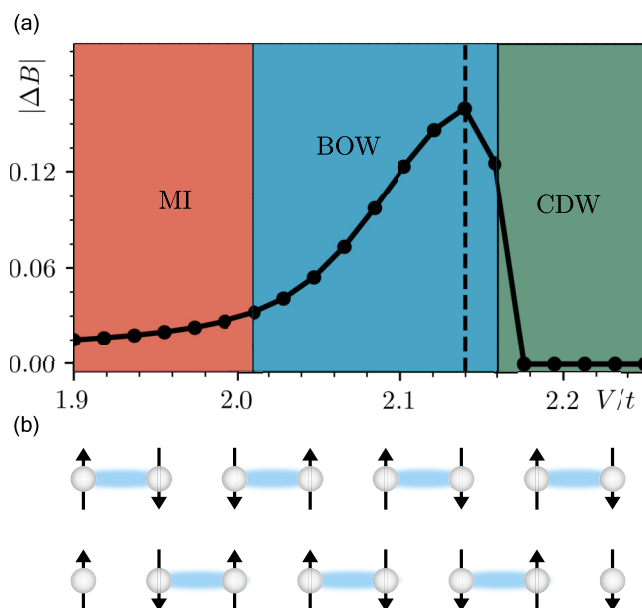


FIG. 1. (a) $|\Delta B|$ at fixed $U = 4t$ and different values of V/t . We use the iDMRG algorithm with a two-site unit cell and a large bond dimension $\chi = 3000$. The dashed line $V/t \simeq 2.14$ corresponds to the maximum value of ΔB . (b) Sketch of the spontaneous dimerization in the BOW phase, with bonds corresponding to a large $|\hat{B}_i|$ depicted in blue. The upper chain corresponds to the trivial case, while the lower chain is topologically nontrivial and exhibits edge states under open boundary conditions.

at $U = 2V$. However, when V and U compete and are comparable to the hopping amplitude t , frustration effects induce a third phase, the fully gapped BOW [28,30–39]. Such a phase is characterized by a uniform distribution of particles, as in MIs, accompanied by a spontaneous dimerization that leads to a staggered expectation value of the bond operator $\hat{B}_i = \frac{1}{2} \sum_{\sigma} (\hat{c}_{i,\sigma}^\dagger \hat{c}_{i+1,\sigma} + \text{H.c.})$ captured by $\Delta B_i \equiv \langle \hat{B}_i - \hat{B}_{i+1} \rangle$. Interestingly, including dipolar interactions beyond the NN term sensibly enlarges the range of parameters where the BOW can be found [39].

Here, we complement previous analyses in finite systems by performing infinite density matrix renormalization group (iDMRG) calculations [74] where boundaries do not play any role, thus allowing one to study only the properties of the bulk of the system. Figure 1(a) shows $|\Delta B| \equiv |\Delta B_{L/2}|$ as a function of V for $U = 4t$: While the BOW-CDW transition can be accurately determined at $V_{\text{BOW-CDW}} \simeq 2.16t$, the Berezinskii-Kosterlitz-Thouless nature of the MI-BOW transition makes it challenging to derive the transition point accurately (see Supplemental Material [75]). Previous finite-size extrapolations of the thermodynamic limit yield $V_{\text{MI-BOW}} \simeq 1.88t$ [33,38]. However, the more recent study of Ref. [76], based on a gap-scaling analysis in finite systems, results in a considerably larger value $V_{\text{MI-BOW}} \simeq 2.08t$. Here, by working directly in the thermodynamic limit, we refine such predictions, and obtain $V_{\text{MI-BOW}} \gtrsim 2.01t$.

Degeneracy of the BOW phase. Our iDMRG calculations allow one to identify an exact bulk degeneracy between the two ground states. Such equivalent bulk solutions correspond to the two bulk sectors of the spontaneously symmetry-broken

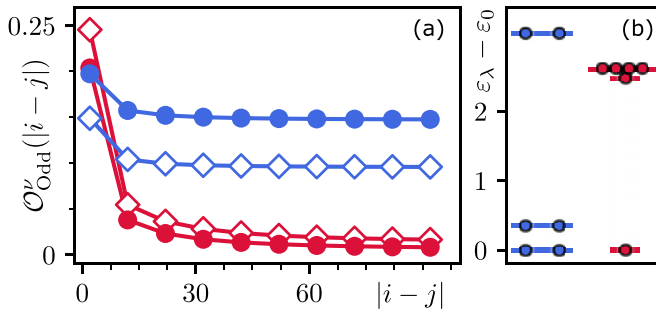


FIG. 2. Topological properties of the BOW at half filling for $U = 4t$ and $V = 2.14t$ obtained with iDMRG. Red (blue) colors are used for the trivial (topological) sectors. (a) Long-range behavior of the odd string order parameters. Solid circles (open squares) are used for the spin (charge) strings. (b) ES energies $\epsilon_\lambda \equiv -\log S_\lambda^2$.

BOW with $\pm|\Delta B|$ [Fig. 1(b)]. Notice that these two degenerate ground states correspond to two effective lattice dimerizations, which are reminiscent of the two possible static dimerizations in the SSH model. Indeed, the behavior of the parity operators in the BOW phase [53] is the same as in the SSH model with on-site repulsion [50]. In what follows, by characterizing the topology of the BOW in the bulk, we confirm that the system realizes a SPT phase protected by chiral and inversion symmetry.

Characterization of the topological bulk sector. For one-dimensional interacting systems, the presence of a SPT phase is signaled by a nonvanishing value of a nonlocal string order parameter [52–54] that can be measured in ultracold atomic systems with a quantum gas microscope [70–73]. In particular, the topological nature of SSH-like chains is captured by the long-range order of the following string correlator [77–79],

$$O_{\text{odd}}^v(|i-j|) = \left| 4 \left\langle \hat{S}_{2i+1}^v \exp \left[i\pi \sum_{k=2i+2}^{2j-1} \hat{S}_k^v \right] \hat{S}_{2j}^v \right\rangle \right|, \quad (2)$$

where $\nu = s, c$ denotes the spin and charge sectors. Due to the fully gapped nature of the BOW phase, we calculate the string correlator (2) both in the spin sector, where $\hat{S}_i^s = \frac{1}{2}(\hat{n}_{i,\uparrow} - \hat{n}_{i,\downarrow})$ and in the charge sector, where $\hat{S}_i^c = \frac{1}{2}(\hat{n}_i - 1)$. Figure 2(a) shows the spin and charge strings of the degenerate ground states. A proper scaling of these quantities allows one to infer the limit of $O_{\text{odd}}^v \equiv \lim_{|i-j| \rightarrow \infty} O_{\text{odd}}^v(|i-j|)$: O_{odd}^s and O_{odd}^c are finite for the gapped topological spin and charge sectors and vanish for the topologically trivial phase. Since the two bulk ground states are identical up to a translation of one site, the even string order $O_{\text{even}}^v(|i-j|) = |4 \langle \hat{S}_{2i}^v \exp[i\pi \sum_{k=2i+1}^{2j} \hat{S}_k^v] \hat{S}_{2j+1}^v \rangle|$ has the opposite property: It is finite in the trivial sector and vanishing in the topological one. Nevertheless, as our goal is to characterize both bulk and edge topological properties, O_{odd}^v is the proper observable to predict the appearance of edge states in finite-size systems.

Moreover, the degeneracy of the ES also allows one to characterize the topology of the degenerate ground states [3,55]: In 1D, it has been shown that, under the preservation of their protecting symmetries, SPT phases exhibit an even degeneracy of the ES, and therefore phases with the same

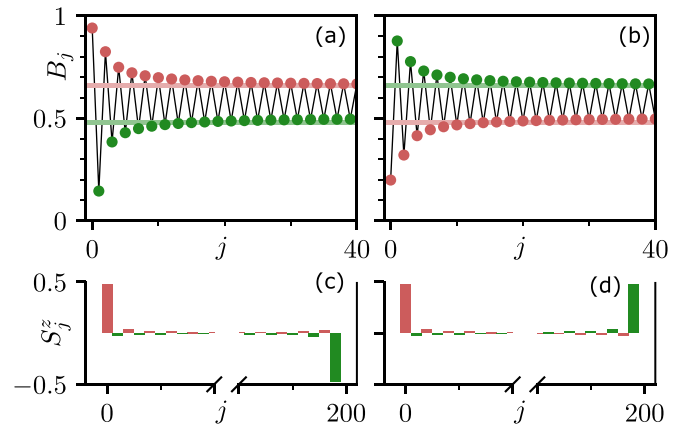


FIG. 3. Finite DMRG results at half filling for $U = 4t$, $V = 2.14t$, $L = 200$, and $\chi_{\text{max}} = 1200$. Red (green) points are used for the even (odd) bonds or sites. (a), (b) Expectation value of the bond operator in the BOW phase exhibiting the trivial (a) and topological (b) staggered patterns. Only the first sites on the left part of the chain are shown, as the bond profile is symmetric with respect to its center. Solid lines represent the iDMRG value with $\chi_{\text{max}} = 3000$. (c), (d) Local polarization of two degenerate topological solutions corresponding to the bond staggerization of (b) for $S_z = 0$ (c) and $S_z = +1$ (d).

ES degeneracy can be connected adiabatically and are thus topologically equivalent. We therefore compute the ES S_λ , given by the eigenvalues of the reduced density matrices for a bipartite cut of the infinite chain. Figure 2(b) shows the ES for the two degenerate iDMRG ground states of the BOW: The BOW is either a trivial phase with a lack of even degeneracy of the ES or a topological phase with an even degenerate spectrum, as in the dimerized SSH-Hubbard model [46–48,50]. The latter is consistent with the previous string order analysis.

Topological edges in finite-size systems. For a finite-size system, border effects break the degeneracy of the two ground states and the topological dimerized pattern turns out to be an excited state for open boundary conditions: In the bulk, the fermions always tunnel to the left/right site with an effective hopping strength $t(1 \pm |\Delta B|)$ but, at the edge of the chain, the system is forced to select the most favorable hopping configuration, namely the one given by $t(1 + |\Delta B_0|)$. Therefore, previous finite DMRG studies of Eq. (1) only focused on the state related to the trivial topology. We now show how such a BOW phase can be stabilized in the presence of edges with finite DMRG. In order to select a given dimerization, we use a local pinning field that fixes the bond pattern at the borders of the chain [75]. Figures 3(a) and 3(b) show the two staggered bond patterns obtained by varying the sign of the pinning field, that correspond to the trivial and topological BOW phase, respectively. Figure 3(c) shows the spin-polarized edge states only appearing in the topological sector. As these edge states couple weakly with the bulk (see Supplemental Material [75]), we can approximate the reduced density matrix of the edges by the product state wave function $|\Psi\rangle_{\text{edges}} = |\cdot\rangle_L |\cdot\rangle_R$, where $|\cdot\rangle_{L(R)}$ represents the quantum state of the first (last) site of the chain. Let us now discuss the degeneracy of such an edge state manifold. In the $\hat{S}_z = 0$ sector, the system has two degenerate topological ground states corresponding to

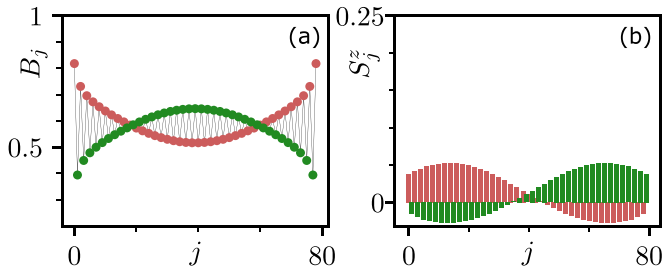


FIG. 4. Finite DMRG results for $U = 4t$, $V = 2.14t$, $L = 80$, and $\chi_{\max} = 1200$, with $S_z = +1$. (a) Solitonic profile in the bond order. (b) Local magnetization profile exhibiting a delocalized spin excitation.

$|\downarrow\rangle_L |\uparrow\rangle_R$ and $|\uparrow\rangle_L |\downarrow\rangle_R$ [see Fig. 3(c)], in accordance with the twofold degeneracy of the ES. Furthermore, as shown in Fig. 3(d), these two ground states also have gapless edge spin excitations: The spin sector $S_z = \pm 1$ exhibits degenerate ground states of the form $|\uparrow\rangle_L |\uparrow\rangle_R$ or $|\downarrow\rangle_L |\downarrow\rangle_R$, respectively. Therefore, the edge state manifold for a finite-size system, including both the $S_z = 0$ and $S_z = \pm 1$ sectors, is fourfold degenerate.

Let us now compare this degeneracy with the well-known case of the SSH model including the Hubbard interaction U , i.e., the SSH-Hubbard model [44–51]. In the limiting case $U = 0$, the SSH topological ground state exhibits a sixfold degeneracy composed by the states $|\uparrow\rangle_L |\downarrow\rangle_R$, $|\downarrow\rangle_L |\uparrow\rangle_R$, $|\uparrow\rangle_L |0\rangle_R$, $|0\rangle_L |\uparrow\rangle_R$ in the $S_z = 0$ sector, and $|\uparrow\rangle_L |\uparrow\rangle_R$, $|\downarrow\rangle_L |\downarrow\rangle_R$ for $S_z = \pm 1$. However, a finite U results in an energy penalty for the states $|\uparrow\rangle_L |0\rangle_R$, $|0\rangle_L |\uparrow\rangle_R$, which become gapped. Hence, the interaction-induced BOW phase exhibits the same edge state manifold as a static dimerized model with on-site interaction U .

Solitonic bulk excitations. Another interesting aspect of the BOW in a finite chain is related to the interplay between spontaneous symmetry breaking and topology when bulk excited states are considered. In noninteracting topological insulators with static dimerizations, such as the SSH model, the excited bulk states are described as gapped modes carrying charge or spin on top of a background with a fixed sector of the dimerization. In contrast, here the dimerization is spontaneously induced via interactions, allowing for solitonic excitations interpolating between the two possible dimerization patterns. We note that, although topological defects also appear in the presence of phononic degrees of freedom [13,80,81], here we observe them for single species through the frustration-induced spontaneous symmetry-breaking mechanism. We focus on bulk spin excitations of the topological BOW at half filling, as the charge gap is significantly larger [38].

Importantly, such excitations also represent a route to obtain the topological sector of the BOW in a finite chain without relying on a pinning mechanism at the borders. This is what is shown in Fig. 4(a), where one can observe the first bulk spin excitation ($S_z = +1$) in the trivial BOW phase. We observe the solitonic domain walls interpolating between the trivial dimerization (left and right borders) to the topological one (central region). Notice that, as shown in Fig. 4(b), this corresponds to a delocalized soliton picture and thus this static solution

is expected to be mobile; the DMRG solution corresponds to the minimum of a soliton band in the spin sector. The latter is reminiscent of a Peierl’s mechanism with quantum phonons, but in the present case the solitons are generated by the same fermionic interactions.

Experimental proposal with ultracold dipolar gases. Hamiltonian (1) can be simulated using a spin mixture in a dipolar Fermi gas of highly magnetic atoms. Since the emergence of the BOW phase is a rather general phenomenon, it can be experimentally investigated using various platforms and under realistic parameters. As an example, we consider lattice-confined fermionic erbium [69] in a rectangular 3D lattice with spacings $(\Delta x, \Delta y, \Delta z) = (266, 266, 532)$ nm and lattice depths $(E_x, E_y, E_z) = (19, 40, 80)E_{\text{rec}}$. This results in tunneling rates $(t_x \equiv t, t_y, t_z) = (12.5, 0.5, 0.001)$ Hz, realizing the required effective 1D chains. Here, E_{rec} is the photon recoil energy. The states $|\uparrow\rangle$ and $|\downarrow\rangle$ can be mapped into the two lowest Er Zeeman states. We find that the BOW phase, i.e., $U/t \sim 4$ and $V/t \gtrsim 2$, can be realized in the experiment with realistic parameters that allow us to match these conditions. For the above lattice parameter and a scattering length of $a_s = 20a_0$ between $|\uparrow\rangle$ and $|\downarrow\rangle$, we indeed calculate $U = 55$ Hz and $V = 28$ Hz. Notice that higher-order terms in the Hamiltonian, such as dipolar interactions beyond nearest neighbors [39], density-induced tunneling [82], or spin-dependent dipolar terms, do not destabilize the BOW phases and its topological phases (see Supplemental Material [75] for an extended discussion).

Magnetic atoms lend themselves very well to all the Hamiltonian manipulation and engineering techniques developed with alkali atoms. This includes preparation of Mott states, spin manipulation, high-resolution imaging, and local control made accessible via microscopic techniques [83]. In addition, the rich atomic spectrum, distinctive of lanthanides [56], allows for new types of ultrafast control of the spin dynamics via optical manipulation based, e.g., on clock-type optical transitions [84,85].

Conclusions. We showed that the BOW induced by frustration between competing couplings has a nontrivial topological sector in the presence of chiral symmetry. To this aim, we analyzed the BOW of the extended Fermi-Hubbard model. We revealed its topological nature by finding a nonzero string order correlator and a degenerate entanglement spectrum. We then discussed strategies to stabilize the topological sector in finite-size systems. The methods proposed in this Letter are general and can be used to analyze the topology of chiral-symmetric BOW phases induced by frustration, which are encountered in very diverse strongly correlated quantum systems. Finally, we also designed a realistic experimental scheme involving magnetic atoms trapped in an optical lattice where the topological BOW phase can be realized. The latter paves the way towards an efficient quantum simulation of topological phases in many-body quantum systems.

Acknowledgments. The ICFO group acknowledges support from ERC AdG NOQIA; Agencia Estatal de Investigación (R&D Project No. CEX2019-000910-S, funded by MCIN/AEI/10.13039/501100011033, Plan National FIDEUA PID2019-106901GB-I00, FPI, QUANTERA MAQS PCI2019-111828-2, QUANTERA DYNAMITE

PCI2022-132919, Proyectos de I + D + I “Retos Colaboración” QUSPIN RTC2019-007196-7), MCIN via European Union NextGenerationEU (PRTR); Fundació Cellex; Fundació Mir-Puig; Generalitat de Catalunya through the European Social Fund FEDER and CERCA program (AGAUR Grant No. 2017 SGR 134, QuantumCAT U16-011424, cofunded by ERDF Operational Program of Catalonia 2014-2020); EU Horizon 2020 FET-OPEN OPTologic (Grant No. 899794); National Science Centre, Poland (Symfonia Grant No. 2016/20/W/ST4/00314); and European Union’s Horizon 2020 research and innovation programme under the Marie-Skłodowska-Curie Grant Agreements No. 101029393 (STREDCH) and No. 847648 (“La Caixa” Junior Leaders fellowships ID100010434: LCF/BQ/PI19/11690013,

LCF/BQ/PI20/11760031, LCF/BQ/PR20/11770012, LCF/BQ/PR21/11840013). S.J.-F. acknowledges financial support from MCIN/AEI/10.13039/501100011033 and FSE “El FSE invierte en tu futuro” (reference code BES-2017-082118). A.D. further acknowledges the financial support from a fellowship granted by la Caixa Foundation (ID 100010434, fellowship code LCF/BQ/PR20/11770012). D.G.-C. is supported by the Simons Collaboration on Ultra-Quantum Matter, which is a grant from the Simons Foundation (651440, P.Z.). The Innsbruck group acknowledges support from a QuantERA grant MAQS from the Austrian Science Fund (FWF No. I4391-N). DMRG calculations were performed using the TeNPy Library [74].

-
- [1] Z.-C. Gu and X.-G. Wen, Tensor-entanglement-filtering renormalization approach and symmetry-protected topological order, *Phys. Rev. B* **80**, 155131 (2009).
- [2] M. Z. Hasan and C. L. Kane, Colloquium: Topological insulators, *Rev. Mod. Phys.* **82**, 3045 (2010).
- [3] F. Pollmann, A. M. Turner, E. Berg, and M. Oshikawa, Entanglement spectrum of a topological phase in one dimension, *Phys. Rev. B* **81**, 064439 (2010).
- [4] X. Chen, Z.-C. Gu, Z.-X. Liu, and X.-G. Wen, Symmetry-protected topological orders in interacting bosonic systems, *Science* **338**, 1604 (2012).
- [5] N. R. Cooper, J. Dalibard, and I. B. Spielman, Topological bands for ultracold atoms, *Rev. Mod. Phys.* **91**, 015005 (2019).
- [6] L. D. Landau, On the theory of phase transitions, *Zh. Eksp. Teor. Fiz.* **7**, 19 (1937).
- [7] C.-K. Chiu, J. C. Y. Teo, A. P. Schnyder, and S. Ryu, Classification of topological quantum matter with symmetries, *Rev. Mod. Phys.* **88**, 035005 (2016).
- [8] A. Kitaev and C. Laumann, Topological phases and quantum computation, in *Exact Methods in Low-Dimensional Physics and Quantum Computing*, edited by J. Jacobsen, S. Ouvry, V. Pasquier, D. Serban, and L. Cugliandolo, Lecture Notes of the Les Houches Summer School, LXXXIX (Oxford University Press, Oxford, U.K., 2009).
- [9] K. von Klitzing, Metrology in 2019, *Nat. Phys.* **13**, 198 (2017).
- [10] M. Lewenstein, A. Sanpera, and V. Ahufinger, *Ultracold Atoms in Optical Lattices: Simulating Quantum Many Body Systems*, 2nd ed. (Oxford University Press, Oxford, 2017).
- [11] I. Bloch, J. Dalibard, and W. Zwerger, Many-body physics with ultracold gases, *Rev. Mod. Phys.* **80**, 885 (2008).
- [12] N. Goldman, J. C. Budich, and P. Zoller, Topological quantum matter with ultracold gases in optical lattices, *Nat. Phys.* **12**, 639 (2016).
- [13] W. P. Su, J. R. Schrieffer, and A. J. Heeger, Solitons in Polyacetylene, *Phys. Rev. Lett.* **42**, 1698 (1979).
- [14] M. Atala, M. Aidelsburger, J. T. Barreiro, D. Abanin, T. Kitagawa, E. Demler, and I. Bloch, Direct measurement of the Zak phase in topological Bloch bands, *Nat. Phys.* **9**, 795 (2013).
- [15] E. J. Meier, F. A. An, and B. Gadway, Observation of the topological soliton state in the Su-Schrieffer-Heeger model, *Nat. Commun.* **7**, 13986 (2016).
- [16] E. J. Meier, F. A. An, A. Dauphin, M. Maffei, P. Massignan, T. L. Hughes, and B. Gadway, Observation of the topological Anderson insulator in disordered atomic wires, *Science* **362**, 929 (2018).
- [17] S. de Léséleuc, V. Lienhard, P. Scholl, D. Barredo, S. Weber, N. Lang, H. P. Büchler, T. Lahaye, and A. Browaeys, Observation of a symmetry-protected topological phase of interacting bosons with Rydberg atoms, *Science* **365**, 775 (2019).
- [18] P. Sompert, S. Hirthe, D. Bourgund, T. Chalopin, J. Bibo, J. Koepsell, P. Bojović, R. Verresen, F. Pollmann, G. Salomon, C. Gross, T. A. Hilker, and I. Bloch, Realising the symmetry-protected Haldane phase in Fermi-Hubbard ladders, *Nature* **606**, 484 (2022).
- [19] R. E. Peierls, *Quantum Theory of Solids* (Clarendon, Oxford, U.K., 1996).
- [20] D. González-Cuadra, P. R. Grzybowski, A. Dauphin, and M. Lewenstein, Strongly Correlated Bosons on a Dynamical Lattice, *Phys. Rev. Lett.* **121**, 090402 (2018).
- [21] D. González-Cuadra, A. Dauphin, P. R. Grzybowski, P. Wójcik, M. Lewenstein, and A. Bermudez, Symmetry-breaking topological insulators in the \mathbb{Z}_2 Bose-Hubbard model, *Phys. Rev. B* **99**, 045139 (2019).
- [22] D. González-Cuadra, A. Bermudez, P. R. Grzybowski, M. Lewenstein, and A. Dauphin, Intertwined topological phases induced by emergent symmetry protection, *Nat. Commun.* **10**, 2694 (2019).
- [23] A. A. Aligia, A. Anfossi, L. Arrachea, C. Degli Esposti Boschi, A. O. Dobry, C. Gazza, A. Montorsi, F. Ortolani, and M. E. Torio, Incommensurability and Unconventional Superconductor to Insulator Transition in the Hubbard Model with Bond-Charge Interaction, *Phys. Rev. Lett.* **99**, 206401 (2007).
- [24] H. Otsuka and M. Nakamura, Ground-state phase diagram of the one-dimensional Hubbard model with an alternating chemical potential, *Phys. Rev. B* **71**, 155105 (2005).
- [25] L. Tincani, R. M. Noack, and D. Baeriswyl, Critical properties of the band-insulator-to-Mott-insulator transition in the strong-coupling limit of the ionic Hubbard model, *Phys. Rev. B* **79**, 165109 (2009).
- [26] K. Hallberg, E. Gagliano, and C. Balseiro, Finite-size study of a spin-1/2 Heisenberg chain with competing interactions: Phase diagram and critical behavior, *Phys. Rev. B* **41**, 9474 (1990).

- [27] P. Schmitteckert and R. Werner, Charge-density-wave instabilities driven by multiple umklapp scattering, *Phys. Rev. B* **69**, 195115 (2004).
- [28] T. Mishra, J. Carrasquilla, and M. Rigol, Phase diagram of the half-filled one-dimensional t - v - V' model, *Phys. Rev. B* **84**, 115135 (2011).
- [29] S. Mondal, A. Padhan, and T. Mishra, Realizing symmetry protected topological phase through dimerized interactions, [arXiv:2202.13966](https://arxiv.org/abs/2202.13966).
- [30] M. Nakamura, Mechanism of CDW-SDW transition in one dimension, *J. Phys. Soc. Jpn.* **68**, 3123 (1999).
- [31] M. Nakamura, Tricritical behavior in the extended Hubbard chains, *Phys. Rev. B* **61**, 16377 (2000).
- [32] E. Jeckelmann, Ground-State Phase Diagram of a Half-Filled One-Dimensional Extended Hubbard Model, *Phys. Rev. Lett.* **89**, 236401 (2002).
- [33] P. Sengupta, A. W. Sandvik, and D. K. Campbell, Bond-order-wave phase and quantum phase transitions in the one-dimensional extended Hubbard model, *Phys. Rev. B* **65**, 155113 (2002).
- [34] A. W. Sandvik, L. Balents, and D. K. Campbell, Ground State Phases of the Half-Filled One-Dimensional Extended Hubbard Model, *Phys. Rev. Lett.* **92**, 236401 (2004).
- [35] Y. Z. Zhang, Dimerization in a Half-Filled One-Dimensional Extended Hubbard Model, *Phys. Rev. Lett.* **92**, 246404 (2004).
- [36] K.-M. Tam, S.-W. Tsai, and D. K. Campbell, Functional Renormalization Group Analysis of the Half-Filled One-Dimensional Extended Hubbard Model, *Phys. Rev. Lett.* **96**, 036408 (2006).
- [37] S. Glocke, A. Klümper, and J. Sirker, Half-filled one-dimensional extended Hubbard model: Phase diagram and thermodynamics, *Phys. Rev. B* **76**, 155121 (2007).
- [38] S. Ejima and S. Nishimoto, Phase Diagram of the One-Dimensional Half-Filled Extended Hubbard Model, *Phys. Rev. Lett.* **99**, 216403 (2007).
- [39] M. Di Dio, L. Barbiero, A. Recati, and M. Dalmonte, Spontaneous Peierls dimerization and emergent bond order in one-dimensional dipolar gases, *Phys. Rev. A* **90**, 063608 (2014).
- [40] R. D. Somma and A. A. Aligia, Phase diagram of the XXZ chain with next-nearest-neighbor interactions, *Phys. Rev. B* **64**, 024410 (2001).
- [41] M. Sato, S. Furukawa, S. Onoda, and A. Furusaki, Competing phases in spin-1/2 J_1 - J_2 chain with easy-plane anisotropy, *Mod. Phys. Lett. B* **25**, 901 (2011).
- [42] M. Kumar, S. Ramasesha, and Z. G. Soos, Bond-order wave phase, spin solitons, and thermodynamics of a frustrated linear spin- $\frac{1}{2}$ Heisenberg antiferromagnet, *Phys. Rev. B* **81**, 054413 (2010).
- [43] T. Mishra, R. V. Pai, S. Mukerjee, and A. Paramekanti, Quantum phases and phase transitions of frustrated hard-core bosons on a triangular ladder, *Phys. Rev. B* **87**, 174504 (2013).
- [44] V. Gurarie, Single-particle Green's functions and interacting topological insulators, *Phys. Rev. B* **83**, 085426 (2011).
- [45] S. R. Manmana, A. M. Essin, R. M. Noack, and V. Gurarie, Topological invariants and interacting one-dimensional fermionic systems, *Phys. Rev. B* **86**, 205119 (2012).
- [46] T. Yoshida, R. Peters, S. Fujimoto, and N. Kawakami, Characterization of a Topological Mott Insulator in One Dimension, *Phys. Rev. Lett.* **112**, 196404 (2014).
- [47] D. Wang, S. Xu, Y. Wang, and C. Wu, Detecting edge degeneracy in interacting topological insulators through entanglement entropy, *Phys. Rev. B* **91**, 115118 (2015).
- [48] B.-T. Ye, L.-Z. Mu, and H. Fan, Entanglement spectrum of Su-Schrieffer-Heeger-Hubbard model, *Phys. Rev. B* **94**, 165167 (2016).
- [49] B. Sierski and C. Karrasch, Topological invariants for the Haldane phase of interacting Su-Schrieffer-Heeger chains: Functional renormalization-group approach, *Phys. Rev. B* **98**, 165101 (2018).
- [50] L. Barbiero, L. Santos, and N. Goldman, Quenched dynamics and spin-charge separation in an interacting topological lattice, *Phys. Rev. B* **97**, 201115(R) (2018).
- [51] N. H. Le, A. J. Fisher, N. J. Curson, and E. Ginossar, Topological phases of a dimerized Fermi-Hubbard model for semiconductor nano-lattices, *npj Quantum Inf.* **6**, 24 (2020).
- [52] M. den Nijs and K. Rommelse, Preroughening transitions in crystal surfaces and valence-bond phases in quantum spin chains, *Phys. Rev. B* **40**, 4709 (1989).
- [53] L. Barbiero, A. Montorsi, and M. Roncaglia, How hidden orders generate gaps in one-dimensional fermionic systems, *Phys. Rev. B* **88**, 035109 (2013).
- [54] A. Montorsi, F. Dolcini, R. C. Iotti, and F. Rossi, Symmetry-protected topological phases of one-dimensional interacting fermions with spin-charge separation, *Phys. Rev. B* **95**, 245108 (2017).
- [55] M. P. Zaletel, R. S. K. Mong, and F. Pollmann, Flux insertion, entanglement, and quantized responses, *J. Stat. Mech.: Theory Exp.* (2014) P10007.
- [56] M. A. Norcia and F. Ferlaino, Developments in atomic control using ultracold magnetic lanthanides, *Nat. Phys.* **17**, 1349 (2021).
- [57] L. Chomaz, S. Baier, D. Petter, M. J. Mark, F. Wächtler, L. Santos, and F. Ferlaino, Quantum-Fluctuation-Driven Crossover from a Dilute Bose-Einstein Condensate to a Macrodroplet in a Dipolar Quantum Fluid, *Phys. Rev. X* **6**, 041039 (2016).
- [58] M. Schmitt, M. Wenzel, F. Böttcher, I. Ferrier-Barbut, and T. Pfau, Self-bound droplets of a dilute magnetic quantum liquid, *Nature (London)* **539**, 259 (2016).
- [59] F. Böttcher, J.-N. Schmidt, M. Wenzel, J. Hertkorn, M. Guo, T. Langen, and T. Pfau, Transient Supersolid Properties in an Array of Dipolar Quantum Droplets, *Phys. Rev. X* **9**, 011051 (2019).
- [60] L. Tanzi, E. Lucioni, F. Famà, J. Catani, A. Fioretti, C. Gabbanini, R. N. Bisset, L. Santos, and G. Modugno, Observation of a Dipolar Quantum Gas with Metastable Supersolid Properties, *Phys. Rev. Lett.* **122**, 130405 (2019).
- [61] L. Chomaz, D. Petter, P. Ilzhöfer, G. Natale, A. Trautmann, C. Politi, G. Durastante, R. M. W. van Bijnen, A. Patscheider, M. Sohmen, M. J. Mark, and F. Ferlaino, Long-Lived and Transient Supersolid Behaviors in Dipolar Quantum Gases, *Phys. Rev. X* **9**, 021012 (2019).
- [62] M. A. Norcia, C. Politi, L. Klaus, E. Poli, M. Sohmen, M. J. Mark, R. N. Bisset, L. Santos, and F. Ferlaino, Two-dimensional supersolidity in a dipolar quantum gas, *Nature (London)* **596**, 357 (2021).
- [63] Y. Tang, W. Kao, K.-Y. Li, S. Seo, K. Mallayya, M. Rigol, S. Gopalakrishnan, and B. L. Lev, Thermalization near

- Integrability in a Dipolar Quantum Newton's Cradle, *Phys. Rev. X* **8**, 021030 (2018).
- [64] C. Trefzger, C. Menotti, B. Capogrosso-Sansone, and M. Lewenstein, Ultracold dipolar gases in optical lattices, *J. Phys. B: At., Mol. Opt. Phys.* **44**, 193001 (2011).
- [65] A. de Paz, A. Sharma, A. Chotia, E. Maréchal, J. H. Huckans, P. Pedri, L. Santos, O. Gorceix, L. Vernac, and B. Laburthe-Tolra, Nonequilibrium Quantum Magnetism in a Dipolar Lattice Gas, *Phys. Rev. Lett.* **111**, 185305 (2013).
- [66] O. Dutta, M. Gajda, P. Hauke, M. Lewenstein, D.-S. Lühmann, B. A. Malomed, T. Sowiński, and J. Zakrzewski, Non-standard Hubbard models in optical lattices: a review, *Rep. Prog. Phys.* **78**, 066001 (2015).
- [67] S. Baier, M. J. Mark, D. Petter, K. Aikawa, L. Chomaz, Z. Cai, M. Baranov, P. Zoller, and F. Ferlaino, Extended Bose-Hubbard models with ultracold magnetic atoms, *Science* **352**, 201 (2016).
- [68] S. Lepoutre, J. Schachenmayer, L. Gabardos, B. Zhu, B. Naylor, E. Maréchal, O. Gorceix, A. M. Rey, L. Vernac, and B. Laburthe-Tolra, Out-of-equilibrium quantum magnetism and thermalization in a spin-3 many-body dipolar lattice system, *Nat. Commun.* **10**, 1714 (2019).
- [69] A. Patscheider, B. Zhu, L. Chomaz, D. Petter, S. Baier, A.-M. Rey, F. Ferlaino, and M. J. Mark, Controlling dipolar exchange interactions in a dense three-dimensional array of large-spin fermions, *Phys. Rev. Research* **2**, 023050 (2020).
- [70] M. Endres, M. Cheneau, T. Fukuhara, C. Weitenberg, P. Schauß, C. Gross, L. Mazza, M. C. Bañuls, L. Pollet, I. Bloch, and S. Kuhr, Observation of correlated particle-hole pairs and string order in low-dimensional Mott insulators, *Science* **334**, 200 (2011).
- [71] T. A. Hilker, G. Salomon, F. Grusdt, A. Omran, M. Boll, E. Demler, I. Bloch, and C. Gross, Revealing hidden antiferromagnetic correlations in doped Hubbard chains via string correlators, *Science* **357**, 484 (2017).
- [72] E. Haller, J. Hudson, A. Kelly, D. A. Cotta, B. Peaudecerf, G. D. Bruce, and S. Kuhr, Single-atom imaging of fermions in a quantum-gas microscope, *Nat. Phys.* **11**, 738 (2015).
- [73] A. Mazurenko, C. S. Chiu, G. Ji, M. F. Parsons, M. Kanász-Nagy, R. Schmidt, F. Grusdt, E. Demler, D. Greif, and M. Greiner, A cold-atom Fermi-Hubbard antiferromagnet, *Nature (London)* **545**, 462 (2017).
- [74] J. Hauschild and F. Pollmann, Efficient numerical simulations with Tensor Networks: Tensor Network Python (TeNPy), *SciPost Phys. Lect. Notes* **5** (2018), doi:10.21468/SciPostPhysLectNotes.5.
- [75] See Supplemental Material at <http://link.aps.org/supplemental/10.1103/PhysRevResearch.4.L032005> for details on the numerical simulations, an extended discussion of the effect of extra Hamiltonian terms in the BOW phase, and the numerical calculation of the experimental Hamiltonian parameters.
- [76] M. Dalmonte, J. Carrasquilla, L. Taddia, E. Ercolessi, and M. Rigol, Gap scaling at Berezinskii-Kosterlitz-Thouless quantum critical points in one-dimensional Hubbard and Heisenberg models, *Phys. Rev. B* **91**, 165136 (2015).
- [77] F. Anfuso and A. Rosch, String order and adiabatic continuity of Haldane chains and band insulators, *Phys. Rev. B* **75**, 144420 (2007).
- [78] H. T. Wang, B. Li, and S. Y. Cho, Topological quantum phase transition in bond-alternating spin- $\frac{1}{2}$ Heisenberg chains, *Phys. Rev. B* **87**, 054402 (2013).
- [79] J. Fraxanet, D. González-Cuadra, T. Pfau, M. Lewenstein, T. Langen, and L. Barbiero, Topological Quantum Critical Points in the Extended Bose-Hubbard Model, *Phys. Rev. Lett.* **128**, 043402 (2022).
- [80] D. González-Cuadra, A. Dauphin, P. R. Grzybowski, M. Lewenstein, and A. Bermudez, Dynamical Solitons and Boson Fractionalization in Cold-Atom Topological Insulators, *Phys. Rev. Lett.* **125**, 265301 (2020).
- [81] D. González-Cuadra, A. Dauphin, P. R. Grzybowski, M. Lewenstein, and A. Bermudez, \mathbb{Z}_n solitons in intertwined topological phases, *Phys. Rev. B* **102**, 245137 (2020).
- [82] O. Jürgensen, F. Meinert, M. J. Mark, H.-C. Nägerl, and D.-S. Lühmann, Observation of Density-Induced Tunneling, *Phys. Rev. Lett.* **113**, 193003 (2014).
- [83] C. Gross and W. S. Bakr, Quantum gas microscopy for single atom and spin detection, *Nat. Phys.* **17**, 1316 (2021).
- [84] N. Petersen, M. Trümper, and P. Windpassinger, Spectroscopy of the 1001-nm transition in atomic dysprosium, *Phys. Rev. A* **101**, 042502 (2020).
- [85] A. Patscheider, B. Yang, G. Natale, D. Petter, L. Chomaz, M. J. Mark, G. Hovhannesian, M. Lepers, and F. Ferlaino, Observation of a narrow inner-shell orbital transition in atomic erbium at 1299 nm, *Phys. Rev. Research* **3**, 033256 (2021).